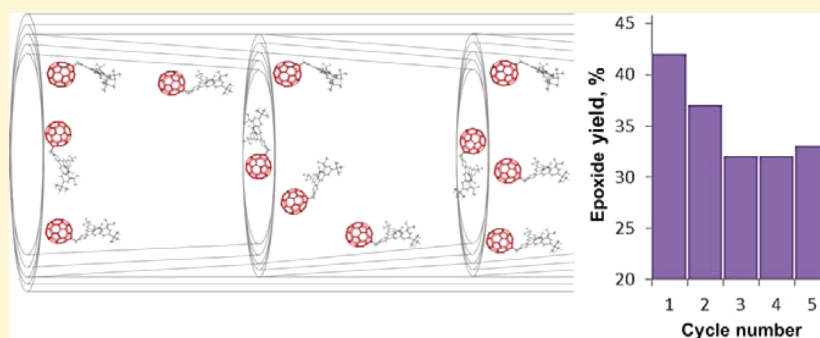


# New Pathway for Heterogenization of Molecular Catalysts by Non-covalent Interactions with Carbon Nanoreactors

Maria A. Lebedeva,<sup>†</sup> Thomas W. Chamberlain,<sup>†</sup> Martin Schröder,<sup>†</sup> and Andrei N. Khlobystov<sup>\*,†,‡</sup>

<sup>†</sup>School of Chemistry, and <sup>‡</sup>Nottingham Nanotechnology and Nanoscience Centre, University of Nottingham, University Park, Nottingham NG7 2RD, United Kingdom

**S** Supporting Information



**ABSTRACT:** A novel approach to heterogenization of catalytic molecules is demonstrated using the nanoscale graphitic step edges inside hollow graphitized carbon nanofibers (GNFs). The presence of the fullerene C<sub>60</sub> moiety within a fullerene–salen Cu<sup>II</sup> complex is essential for anchoring the catalyst within the GNF nanoreactor as demonstrated by comparison to the analogous catalyst complex without the fullerene group. The presence of the catalyst at the step edges of the GNFs is confirmed by high-resolution transmission electron microscopy (TEM) and energy-dispersive X-ray spectroscopy (EDX) with ultraviolet/visible (UV/vis) spectroscopy, demonstrating only negligible (ca. 3%) desorption of the fullerene–salen Cu<sup>II</sup> complex from the GNFs into solution under typical reaction conditions. The catalyst immobilized in GNFs shows good catalytic activity and selectivity toward styrene epoxidation, comparable to the analogous catalyst in solution. Moreover, the fullerene–salen Cu<sup>II</sup> complex in GNFs demonstrates excellent stability and recyclability because it can be readily separated from the reaction mixture and employed in multiple reaction cycles with minimal loss of activity, which is highly advantageous compared to catalysts not stabilized by the graphitic step edges that desorb rapidly from GNFs.

## INTRODUCTION

The ability to separate and recycle the metal catalyst from reaction mixtures without excessive purification steps is crucial for sustainable transition-metal-based catalysis.<sup>1</sup> Recyclability of catalysts can be enhanced by heterogenization of the catalyst molecules, achieved by immobilization on solid supports. This improves the stability of the molecular catalyst and, moreover, renders it insoluble in commonly used organic solvents, thus offering a straightforward separation of the catalyst from the reaction mixture.<sup>2</sup> Heterogenization of a molecular catalyst can be achieved by immobilization on a variety of supports using covalent or non-covalent binding between the catalyst molecules and the support material. The preparation of covalently linked catalysts can be synthetically very demanding, requiring the preparation of non-symmetric ligands bearing functional groups that can form chemical bonds with the support material.<sup>3</sup> On the other hand, non-covalent immobilization can, in principle, be achieved more readily and results in the formation of materials in which the structure and the intrinsic properties of the molecular catalyst are retained. Non-covalent catalyst binding has been achieved in a variety of ways,

including immobilization of catalysts on organic and inorganic supports, such as polystyrenes and other polymers,<sup>4</sup> silica,<sup>5</sup> mesoporous materials,<sup>6</sup> and zeolites,<sup>7</sup> by trapping the catalyst molecules inside porous hosts,<sup>8</sup> and via formation of hydrogen bonds, metal coordination,<sup>9</sup> or electrostatic interactions<sup>10</sup> between the catalyst molecule and the support material.

Non-covalent heterogenization of molecular catalysts also presents several important challenges. Non-covalent interactions are usually reversible, resulting in the gradual loss of the catalytic activity upon recycling.<sup>11</sup> Hence, a good anchoring group is required to provide sufficient binding of the catalyst to the surface of the support to afford high stability of the resulting heterogeneous material. Additionally, non-covalent interactions often lower the degree of control over the location of the catalyst molecules on the support surface. Carbon nanostructures, such as carbon nanotubes (CNTs) and graphite, have been used extensively as robust supporting materials for

Received: August 14, 2014

Revised: October 20, 2014

immobilization of catalysts on both internal and external surfaces and provide excellent stability and thermal and electric conductivity. For example, extended conjugated systems of  $sp^2$  carbons of CNTs and graphite allow for catalyst molecules tagged with polyaromatic hydrocarbons, such as pyrene, to be anchored to the surface using  $\pi$ - $\pi$  stacking interactions.<sup>12</sup> However, such anchoring is relatively weak, low-directional, and not site-specific, with the catalyst deposited randomly over the carbon surface.

In this study, we report a new methodology for heterogenization of transition metal catalysts by tagging them with a fullerene group, which allows for reliable and site-specific anchoring inside graphitized carbon nanofibers (GNFs) via strong van der Waals interactions between the fullerene cage and the internal graphitic step edges of GNFs. The spherical shape and large  $\pi$ -electron system of functionalized  $C_{60}$  fullerenes is known to have a high affinity for  $sp^2$ -hybridized carbon structures and is an excellent match for the preferential binding at graphitic step edges rather than the flat terrace of the inner surface of the GNF support.<sup>13</sup> We demonstrate herein that non-covalent immobilization of a fullerene-tagged [Cu(salen)] catalyst inside GNF nanoreactors can be used to form well-defined heterogeneous catalysts with molecules located in a very distinct, confined environment. These heterogeneous catalysts exhibit enhanced stability and recyclability, while retaining the activity and selectivity of the individual catalytic centers.

## EXPERIMENTAL SECTION

Compounds **1** and **2** were synthesized according to the previously reported procedures.<sup>15</sup> GNFs (PR19 Pyrograf, chemical vapor deposition) were thermally annealed at 400 °C for 30 min prior to use. Styrene was passed through neutral alumina shortly before all reactions. All other reagents and solvents were purchased from Sigma-Aldrich and used without further purification. Reactions were carried out under an aerobic atmosphere and monitored by  $^1H$  nuclear magnetic resonance (NMR) spectroscopy.  $^1H$  NMR spectra were recorded using a Bruker DPX 300 spectrometer. Ultraviolet/visible (UV/vis) spectra were measured using a Lambda 25 PerkinElmer spectrometer.

**Preparation of Heterogeneous Catalysts 1@GNF and 2@GNF.** GNFs (5 mg) were annealed at 400 °C for 30 min and immersed into a solution of the corresponding [Cu(salen)] complex (**1**, 0.2 mg, 0.16  $\mu$ mol or **2**, 0.1 mg, 0.16  $\mu$ mol) in tetrahydrofuran (THF) (2 mL). The mixture was treated by ultrasound and stirred for 30 min, and the solvent was slowly removed under reduced pressure. A new portion of THF (2 mL) was added, and the procedure was repeated 4 times to ensure complete encapsulation of the molecules in GNFs. Upon completion, the **1**@GNF and **2**@GNF catalysts were dried under vacuum for 20 h.

**High-Resolution Transmission Electron Microscopy (HRTEM) Characterization.** HRTEM imaging was performed using a JEOL 2100F transmission electron microscope (field emission electron gun, information limit of 0.19 nm) using an accelerating voltage of 200 kV. Transmission electron microscopy (TEM) specimens were prepared by casting several drops of a methanolic suspension of **1**@GNF or **2**@GNF onto a nickel TEM specimen grid mounted "lacey" carbon film and dried under a stream of nitrogen. Energy-dispersive X-ray (EDX) spectra were recorded for isolated nanofibers of **1**@GNF or **2**@GNF using an Oxford Instruments X-ray detector at 200 kV.

**Leaching Test.** **1**@GNF (5 mg, 0.16  $\mu$ mol of Cu complex) or **2**@GNF (5 mg, 0.16  $\mu$ mol of Cu complex) was immersed in MeCN (4 mL) and heated to 50 °C in a sealed UV/vis cell, and absorption spectra of the resulting solution were measured every 10 min.

**Styrene Epoxidation.** The catalyst (**1**, 0.2 mg, 0.16  $\mu$ mol; **2**, 0.1 mg, 0.16  $\mu$ mol; **1**@GNF, 5 mg, 0.16  $\mu$ mol; **2**@GNF, 5 mg, 0.16  $\mu$ mol;

or GNF, 5 mg) was dissolved or suspended in MeCN (1 mL) containing styrene (52 mg, 0.5 mmol), and a solution of  $t$ BuOOH in nonane (5.5 M, 0.27 mL, 1.5 mmol) was added. The reaction mixture was heated to 80 °C for 7 h, and aliquots of the reaction mixture were then analyzed by  $^1H$  NMR spectroscopy in  $CDCl_3$  solution after each hour without further purification. All quoted reaction yields are a result of at least three repeat reactions.

Styrene, **a**:  $^1H$  NMR (300 MHz,  $CDCl_3$ )  $\delta$ : 7.30–7.50 (m, 5H, Ar H), 6.69 (dd,  $J$  = 17.6 and 10.9 Hz, 1H,  $CH=CH_2$ ), 5.72 (d,  $J$  = 17.6 Hz, 1H,  $CH=CH_2$ ), 5.22 (d,  $J$  = 10.9 Hz, 1H,  $CH=CH_2$ ).

Styrene epoxide, **b**:  $^1H$  NMR (300 MHz,  $CDCl_3$ )  $\delta$ : 7.30–7.50 (m, 5H, Ar H), 3.86 (m, 1H,  $-CH(O)-$ ), 3.15 (dd,  $J$  = 5.5 and 4.1 Hz, 1H,  $CH(O)-CH_2$ ), 2.80 (dd,  $J$  = 5.5 and 2.6 Hz, 1H,  $CH(O)-CH_2$ ).

**c**:  $^1H$  NMR (300 MHz,  $CDCl_3$ )  $\delta$ : 7.20–7.40 (m, 5H, Ar H), 5.28 (dd,  $J$  = 8.0 and 3.6 Hz, 1H), 4.08–4.24 (m, 2H).

**d**:  $^1H$  NMR (300 MHz,  $CDCl_3$ )  $\delta$ : 7.20–7.40 (m, 5H, Ar H), 5.03 (d,  $J$  = 7.7 Hz, 1H), 4.08–4.24 (m, 2H).

**e**:  $^1H$  NMR (300 MHz,  $CDCl_3$ )  $\delta$ : 10.02 (s, 1H,  $CH=O$ ), 7.20–7.40 (m, 5H, Ar H), 5.09 (s, 2H).

**Leaching Test under Catalytic Conditions.** The catalyst (**1**@GNF, 2.5 mg, 0.08  $\mu$ mol or **2**@GNF, 2.5 mg, 0.08  $\mu$ mol) was suspended in MeCN (0.5 mL) containing styrene (26 mg, 0.25 mmol), and in some cases, a solution of  $t$ BuOOH in nonane (5.5 M, 0.13 mL, 1.5 mmol) was added. The reaction mixture was heated to 80 °C for 7 h and filtered hot to remove the insoluble materials. The filtrate was then diluted to 5 mL and analyzed using UV/vis spectroscopy.

**Recyclability Test.** Styrene epoxidation was performed as described above. After the reaction mixture was heated to 80 °C for 7 h, the reaction mixture was allowed to cool to room temperature and the catalyst was removed by filtration, washed extensively with cold  $CH_3CN$  (20 mL), and dried under vacuum for 20 h. The resulting material was then used in the next catalytic cycle.

## RESULTS AND DISCUSSION

Transition metal complexes of salen derivatives are established as highly successful and versatile catalysts. The scope of reactions catalyzed by metal-salen complexes is extremely wide and includes carbon-carbon bond formation, heteroatom-heteroatom bond formation, and carbon-heteroatom bond formation reactions.<sup>14</sup> We have synthesized the fullerene-tagged  $Cu^{II}$  salen complex **1** (Figure 1) in six steps according to our

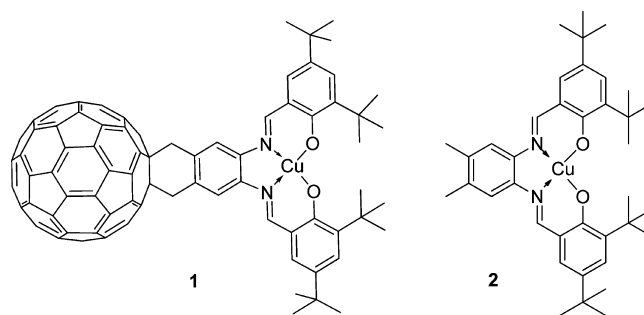


**Figure 1.** Structure of the fullerene-derivatized [Cu(salen)] complex (**1**) and its fullerene-free analogue (**2**).

recently reported procedure.<sup>15</sup> The analogous fullerene-free complex **2** was prepared for comparison. [Cu<sup>II</sup>(salen)] complexes are known to catalyze epoxidation reactions of alkenes, and it has been demonstrated previously that a slight enhancement of the catalytic activity of the transition metal complex is observed upon addition of the fullerene cage because of the electron-withdrawing nature of the carbon cage.<sup>15</sup>

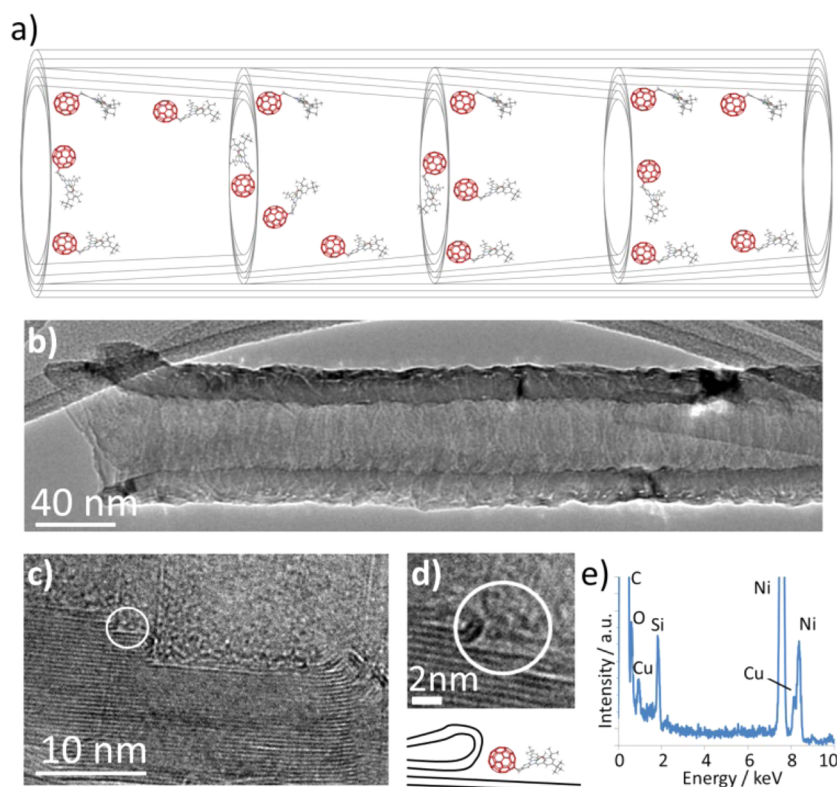


**Figure 2.** (a) Schematic representation of **1@GNF** showing fullerene-containing molecules located preferentially on the step edges of the GNF (fullerene molecules and GNF are not drawn to scale). TEM images of **1@GNF** show (b) the accessible internal channel of the nanoreactor, (c) the internal surface of a GNF filled with **1** (white circle), and (d) a high-magnification TEM image of **1@GNF** showing an individual molecule of **1** located on the step edge of the GNF (top) and its schematic representation (bottom). (e) EDX spectroscopy confirms the presence of copper within the **1@GNF** structure (the Ni peaks are due to the TEM specimen grid).

Immobilization and encapsulation of fullerene-containing molecules inside single-, double-, and multi-walled CNTs has been extensively studied, and the procedure to achieve high filling yields is now well-established.<sup>16</sup> In contrast, GNFs have not been used widely for fullerene encapsulation because of their very wide internal diameters (50–70 nm). However, the structure of GNF consists of stacked truncated cones of graphite layers, and this creates a sequence of step edges (Figure 2a), which are ideally suited to accommodate catalyst molecules. Indeed, it has been demonstrated previously for various metal nanoparticles that guest species are located predominantly on these step-edge sites.<sup>17–19</sup> Furthermore, the diameters of GNFs are sufficiently large to minimize diffusion resistance of the reactant and product molecules to and from the catalytic centers.

The heterogeneous catalyst, **1@GNF**, was prepared by introducing the fullerene-tagged molecules into the internal channel of GNF using a solution method. Initially, the GNFs were thermally treated at 400 °C to remove any residual water molecules from their internal channels and then immersed into a saturated solution of **1** in THF, followed by slow removal of the solvent under reduced pressure to deposit the molecules onto the GNF. Fresh solvent was then added to dissolve any molecules on the outside surface of the GNF, and this procedure was repeated several times to ensure a high degree of pore filling. Immobilization of control compound **2** into GNF was carried out using the same method. The structures of the resultant composite materials (**1@GNF** and **2@GNF**; Figure 2a) were analyzed by HRTEM (panels b and c of Figure 2). HRTEM images of **1@GNF** show the presence of the

individual fullerene-containing molecules (Figure 2c, observed as circles with a diameter of ca. 0.7 nm) located on the internal step edges of the GNF, so that the surface of contact between the C<sub>60</sub> moiety and the step edge of GNF is maximized (Figure 2d). The presence of the [Cu(salen)] moiety is more difficult to visualize because the majority of organic molecules rapidly decompose under the electron beam of TEM. However, the presence of copper inside the GNF was confirmed by localized EDX spectroscopy (Figure 2e). The structure of **2@GNF** was also analyzed by HRTEM, and although fullerene-free molecules were not resolved in the micrograph, the presence of the copper-containing species was also confirmed by EDX.

This procedure enables deposition of the molecules predominantly on the inside of the GNF and also enables precise control of the total amount of catalyst loaded into the GNF support. The catalyst loading in both **1@GNF** and **2@GNF** was 0.03 mmol of copper salen catalyst/g of GNF, which is comparable to similar immobilized metal catalysts in CNTs attached using either covalent<sup>20–22</sup> or non-covalent bonding.<sup>23,24</sup> Table S1 of the Supporting Information compares the catalyst loading in the present study with systems reported previously. The efficiency of the catalyst immobilization in GNFs was quantified by comparing the amount of catalyst that leached from the GNFs into solution over time (Figure 3). The same amount of freshly prepared **1@GNF** or **2@GNF** with identical catalyst loading was immersed in an excess of MeCN and heated to 50 °C in a sealed vessel. The resulting solution was analyzed by UV/vis spectroscopy over time (Figure 3). The majority of the fullerene-containing molecules (97%) was retained in the GNF, giving an almost colorless solution (left

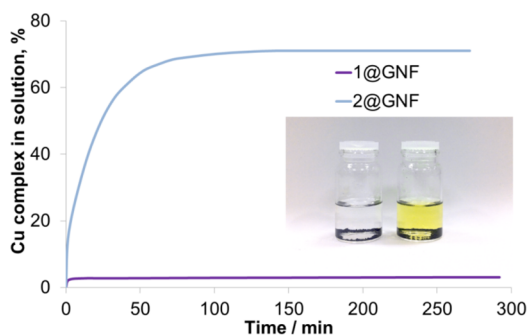


**Figure 3.** Plot showing the amount of the metal complex leached into MeCN at 50 °C over time for 1@GNF (purple line) and 2@GNF (blue line). The inset shows photographs of the resultant mixtures of 1@GNF (left) and 2@GNF (right) in MeCN after 5 h.

inset in Figure 3). In comparison, the fullerene-free complex 2 rapidly leached from the GNF support to form a bright yellow solution (right inset in Figure 3), with only 30% of the initial complex retained in the GNF after 5 h. This confirms that attachment of the fullerene cage to the active [Cu(salen)] catalyst has a dramatic effect on host–guest interactions within the pores of the support and, consequently, the stability of the resulting composite materials.

The performance of the heterogeneous catalysts 1@GNF and 2@GNF was compared in a model styrene epoxidation reaction along with the molecules 1 and 2 under homogeneous

**Scheme 1. Epoxidation of Styrene (a) by <sup>t</sup>BuOOH in the Presence of [Cu(salen)] Forming Styrene Epoxide (b), 1-Phenyl-1,2-bis-*tert*-butylperoxy Ether (c), 1-Phenyl-1-*tert*-butylperoxy-2-*tert*-butyloxy Ether (d), and 2-Phenylacetaldehyde (e)**

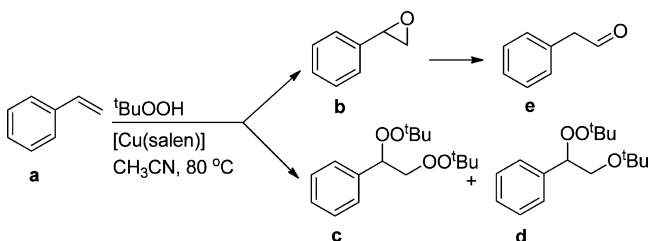


**Table 1. Catalytic Epoxidation of Styrene with <sup>t</sup>BuOOH in MeCN at 80 °C Showing the Distribution of Compounds a–e after 7 h**

catalyst	yield (%)				
	a	b	c	d	e
1	0	46 ± 2	15 ± 2	29 ± 2	10 ± 2
2	0	42 ± 2	26 ± 2	20 ± 2	12 ± 1
1@GNF	0	42 ± 2	19 ± 2	29 ± 2	10 ± 1
2@GNF	0	43 ± 1	14 ± 1	31 ± 2	12 ± 1
GNF	16 ± 2	8 ± 1	50 ± 2	22 ± 2	4 ± 0.5
no catalyst	46 ± 3	2 ± 0.5	39 ± 2	12 ± 1	1 ± 0.5

conditions (Scheme 1 and Table 1). Styrene was reacted with <sup>t</sup>BuOOH in dry MeCN at 80 °C under an aerobic atmosphere, and the reaction mixture was monitored over time by <sup>1</sup>H NMR spectroscopy. The reaction gives a distribution of four different products (Scheme 1), with the target epoxide **b** undergoing further transformations to form the corresponding aldehyde **e**

and radical addition products **c** and **d**. The formation of epoxide is promoted by Cu<sup>II</sup> centers via formation of a Cu<sup>III</sup> peroxy metalocycle intermediate, which then breaks to yield the styrene oxide and regenerate the Cu<sup>II</sup> complex.<sup>25</sup>

Indeed, in the absence of catalyst, only 2% of styrene epoxide is formed (compound **b** in Scheme 1 and Table 1) and the major products are compounds **c** (39%) and **d** (12%) (Scheme 1), formed as a result of an undesirable radical addition of *tert*-butyl peroxy radicals to the double bond of styrene.<sup>26</sup> In the presence of empty GNFs, a similar trend is observed in which the epoxide **b** is a minor product (8% yield) and formation of compounds **c** and **d** is favored (50 and 22%, respectively). Introducing catalysts 1 or 2 promotes epoxide formation, preferentially forming product **b** (42–46%) rather than **c** (15–26%) and **d** (29–20%). This activity and selectivity are comparable to the majority of catalytic systems reported before for styrene epoxidation (see Table S2 of the Supporting Information). The formation of **e**, which is a product of rearrangement of epoxide **b**, depends upon the amount of epoxide in the reaction mixture. However, it is always a minor product, and the total yield of **e** only reaches a maximum of ~10%. The yield and rate of the reaction catalyzed by fullerene-containing complex 1 is slightly higher than the reaction catalyzed by fullerene-free complex 2 (green and orange curves, respectively, in Figure 4). This is the result of the electron-

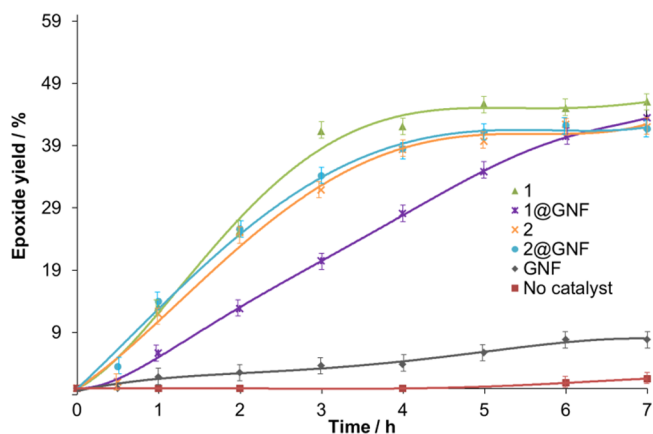


**Figure 4.** Rate of formation of styrene epoxide from styrene in the presence of 1 (green), 2 (orange), 1@GNF (purple), 2@GNF (blue), and GNF (gray) and in the absence of catalyst (red).

withdrawing effect of the fullerene cage depleting the electron density on the Cu<sup>II</sup> center and promoting its catalytic activity, consistent with previous observations.<sup>15</sup>

Complete conversion of styrene **a** and a 42% yield of epoxide **b** is achieved in the presence of the heterogeneous catalyst 1@GNF in 7 h, an outcome very similar to the homogeneous reaction. The heterogeneously catalyzed reaction, however, occurs noticeably slower than the reaction in solution (purple and green curves, respectively, in Figure 4). This is attributed to the fact that the catalytic centers are less accessible in 1@GNF because of the confinement inside the GNF nanoreactor. As a result, complete conversion of styrene and formation of similar amounts of styrene epoxide are achieved over a slightly longer period compared to the solution reaction (Figure 4). This difference in the reaction rates of 1 and 1@GNF also confirms that the catalyst molecules remain immobilized on the GNF throughout the whole process under these conditions. In comparison, under the same reaction conditions, 2@GNF

shows a nearly identical rate of formation of styrene epoxide to **2** in solution (orange and blue curves, respectively, in Figure 4), indicating that both reactions occur in solution under homogeneous conditions. Similar trends are observed for the kinetic curves for styrene conversion and for selectivity for styrene epoxide monitored over time (see Figures S2 and S3 of the Supporting Information).

These trends are further supported by the UV/vis spectroscopy measurements of the reaction mixtures under catalytic conditions. Leaching tests were carried out in the absence of <sup>t</sup>BuOOH to simplify quantitative measurements (see the Supporting Information for details) but in otherwise identical conditions to the catalytic reaction, and these confirm that the majority of the catalyst is leached out of **2**@GNF into solution as a result of only weak interactions between **2** and the GNF. In contrast, 97% of molecules of **1** are retained on GNF (see Figure S5 and Table S3 of the Supporting Information).

To highlight the excellent stability of this heterogeneous catalytic system formed using non-covalent interactions between the fullerene-tagged **1** and GNF, we studied the recyclability of **1**@GNF over a number of repeat catalytic cycles. We tested the performance of **1**@GNF and **2**@GNF in five consecutive epoxidation reactions of styrene (Figure 5),

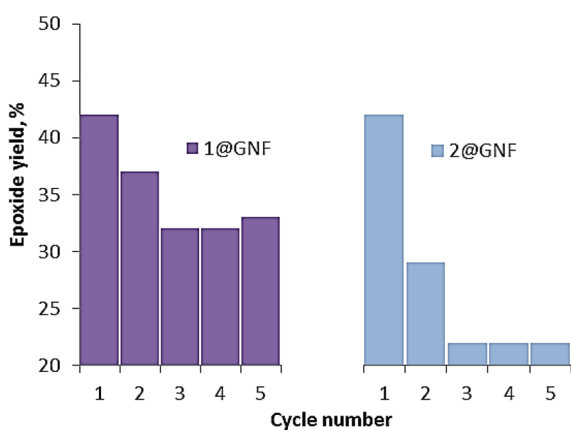


**Figure 5.** Comparison of the stability and recyclability of the catalyst in **1**@GNF (purple) and **2**@GNF (blue) in five consecutive epoxidation reaction cycles of styrene for 7 h.

with each cycle lasting 7 h. The catalyst was separated from the reaction mixture after each cycle by filtration, extensively washed with MeCN to remove any traces of the reactants/products, and used in the next otherwise identical reaction cycle. The conversion of styrene was 100% for the first catalytic cycle in each case. An identical 42% yield of epoxide was achieved for both catalysts in the first cycles of catalysis. However, the catalytic activity of **2**@GNF shows a significant drop in the second cycle, forming only 27% of styrene epoxide (blue columns in Figure 5), whereas the fullerene-containing **1**@GNF affords a 37% yield of styrene epoxide (purple columns in Figure 5). A further decrease in activity is observed for **2**@GNF, showing only 22% yield of epoxide after 5 cycles, whereas in the presence of **1**@GNF, even after 5 cycles, the yield of epoxide remains significantly higher and stabilizes at 34% yield. These results confirm the excellent stability of **1**@GNF, in which the catalytic centers are retained on the support material for a longer time. In addition, spatial separation of the fullerene-tagged metal complex on the GNF step edges may also prevent decomposition of the catalyst molecules, which can

occur in solution because of both epoxidation/polymerization of the fullerene cage and dimerization of the [Cu(salen)] complex, leading to the formation of inactive dimeric species and aggregates<sup>27</sup> under an aerobic atmosphere at elevated temperatures.

## CONCLUSION

A non-covalent supramolecular approach for the heterogenization of molecular catalysts has been developed using the unique affinity of C<sub>60</sub> fullerene for carbon nanostructures. A fullerene-tagged [Cu(salen)] complex has been incorporated into GNFs to form robust and stable catalytically active nanostructures. Fullerene–GNF interactions are sufficiently strong to allow for the catalyst molecules to be retained in the GNFs when heated in MeCN over many hours. As a result, this material possesses excellent recyclability while showing a significantly better activity compared to a catalyst without fullerene over multiple reaction cycles.

Synthetic methodologies to tag a variety of transition metal complexes with a fullerene cage,<sup>28</sup> including various bipyridine,<sup>29</sup> terpyridine,<sup>30</sup> and porphyrin<sup>31</sup> complexes, have been extensively developed in the past decade, enabling our methodology to be expanded to a variety of other existing catalytic systems. The enhanced catalyst recyclability achieved in GNFs can be particularly valuable for processes involving rare metals, such as Ru, Os, Pd, Pt, Ag, and Au, and has the potential to significantly lower the cost of their usage in industrial processes.

## ASSOCIATED CONTENT

### Supporting Information

Additional <sup>1</sup>H NMR spectra, UV/vis absorption spectra, styrene epoxidation kinetic curves, and additional literature data. This material is available free of charge via the Internet at <http://pubs.acs.org>.

## AUTHOR INFORMATION

### Corresponding Author

\*E-mail: [andrei.khlobystov@nottingham.ac.uk](mailto:andrei.khlobystov@nottingham.ac.uk)

### Notes

The authors declare no competing financial interest.

## ACKNOWLEDGMENTS

This work was supported by the European Research Council (ERC) (Consolidator Grant to Andrei N. Khlobystov and Advanced Grant to Martin Schröder), the Engineering and Physical Sciences Research Council (EPSRC), and the University of Nottingham.

## REFERENCES

- (1) Corma, A.; Garcia, H. *Chem. Rev.* **2002**, *102*, 3837.
- (2) Baleizão, C.; Garcia, H. *Chem. Rev.* **2006**, *106*, 3987.
- (3) (a) Kim, J. H.; Kim, G. J. *Catal. Lett.* **2004**, *92*, 123. (b) Park, D. W.; Choi, S. D.; Choi, S. J.; Lee, C. Y.; Kim, G. J. *Catal. Lett.* **2002**, *78*, 145.
- (4) Lu, J.; Toy, P. *Chem. Rev.* **2009**, *109*, 815.
- (5) (a) Choudary, B.; Ramani, T.; Maheswaran, H.; Prashant, L.; Ranganath, K.; Kumar, K. *Adv. Synth. Catal.* **2006**, *348*, 493. (b) Kantam, M.; Ramani, T.; Chakrapani, L.; Choudary, B. *J. Mol. Catal. A: Chem.* **2007**, *274*, 11.
- (6) Serrano, D.; Aguado, J.; Vargas, C. *Appl. Catal., A* **2008**, *335*, 172.
- (7) Guo, X.-F.; Kim, Y.-S.; Kim, G.-J. *Top. Catal.* **2009**, *52*, 153.
- (8) Corma, A.; Garcia, H. *Eur. J. Inorg. Chem.* **2004**, 1143.

- (9) Baleizao, C.; Gigante, B.; Sabater, M. J.; Garcia, H.; Corma, A. *Appl. Catal., A* **2002**, *228*, 279.
- (10) Bhattacharjee, S.; Anderson, J. A. *Chem. Commun.* **2004**, 554.
- (11) (a) Das, P.; Silva, A. R.; Carvalho, A. P.; Pires, J.; Freire, C. *Colloids Surf., A* **2008**, *329*, 190. (b) Bai, R.; Fu, X.; Bao, H.; Ren, W. *Catal. Commun.* **2008**, *9*, 1588. (c) Ren, W.; Fu, X.; Bao, H.; Bai, R.; Ding, P.; Sui, B. *Catal. Commun.* **2009**, *10*, 788. (d) Gong, B.; Fu, X.; Chen, J.; Li, Y.; Zou, X.; Tu, X.; Ding, P.; Ma, L. *J. Catal.* **2009**, *262*, 9.
- (12) (a) Liu, G.; Wu, B.; Zhang, J.; Wang, X.; Shao, M.; Wang, J. *Inorg. Chem.* **2009**, *48*, 2383. (b) Li, F.; Zhang, B.; Li, X.; Jiang, Y.; Chen, L.; Li, Y.; Sun, L. *Angew. Chem., Int. Ed.* **2011**, *50*, 12276. (c) Xing, L.; Xie, J.-H.; Chen, Y.-S.; Wang, L.-X.; Zhou, Q.-L. *Adv. Synth. Catal.* **2008**, *350*, 1013. (d) Tran, P.; Le Goff, A.; Heidkamp, J.; Joussemme, B.; Guillet, N.; Palacin, S.; Dau, H.; Fontecave, M.; Artero, V. *Angew. Chem., Int. Ed.* **2011**, *50*, 1371. (e) Vriamont, C.; Devillers, M.; Riant, O.; Hermans, S. *Chem.—Eur. J.* **2013**, *19*, 12009.
- (13) Chamberlain, T. W.; Popov, A. M.; Knizhnik, A. A.; Samoilov, G. E.; Khlobystov, A. N. *ACS Nano* **2010**, *4*, 5203.
- (14) Zulauf, A.; Mellah, M.; Hong, X.; Schulz, E. *Dalton Trans.* **2010**, *39*, 6911.
- (15) Lebedeva, M. A.; Chamberlain, T. W.; Davies, E. S.; Mancel, D.; Thomas, B. E.; Suetin, M.; Bichoutskaia, E.; Schröder, M.; Khlobystov, A. N. *Chem.—Eur. J.* **2013**, *19*, 11999.
- (16) (a) Chamberlain, T. W.; Pfeiffer, R.; Peterlik, H.; Kuzmany, H.; Zerbetto, F.; Melle-Franco, M.; Staddon, L.; Champness, N. R.; Briggs, G. A. D.; Khlobystov, A. N. *Small* **2008**, *4*, 2262. (b) Chamberlain, T. W.; Camenisch, A.; Champness, N. R.; Briggs, G. A. D.; Benjamin, S. C.; Ardavan, A.; Khlobystov, A. N. *J. Am. Chem. Soc.* **2007**, *129*, 8609. (c) Gimenez-Lopez, M. C.; Chuvilin, A.; Kaiser, U.; Khlobystov, A. N. *Chem. Commun.* **2011**, *47*, 2116. (d) Chamberlain, T. W.; Champness, N. R.; Schröder, M.; Khlobystov, A. N. *Chem.—Eur. J.* **2011**, *17*, 668.
- (17) La Torre, A.; Fay, M. W.; Rance, G. A.; Giménez-López, M. C.; Solomonsz, W. A.; Brown, P. D.; Khlobystov, A. N. *Small* **2012**, *8*, 1222.
- (18) Solomonsz, W. A.; Rance, G. A.; Suetin, M.; La Torre, A.; Bichoutskaia, E.; Khlobystov, A. N. *Chem.—Eur. J.* **2012**, *18*, 13180.
- (19) La Torre, A.; Giménez-López, M. C.; Fay, M. W.; Rance, G. A.; Solomonsz, W. A.; Chamberlain, T. W.; Brown, P. D.; Khlobystov, A. N. *ACS Nano* **2012**, *6*, 2000.
- (20) Baleizão, C.; Gigante, B.; Garcia, H.; Corma, A. *Tetrahedron* **2004**, *60*, 10461.
- (21) Nooraiepour, M.; Moghadam, M.; Tangestaninejad, S.; Mirkhani, V.; Mohammadpoor-Baltork, I.; Irvani, N. *J. Coord. Chem.* **2012**, *65*, 226.
- (22) Zakeri, M.; Moghadam, M.; Mohammadpoor-Baltork, I.; Tangestaninejad, S.; Mirkhani, V.; Khosropour, A. R. *J. Coord. Chem.* **2012**, *65*, 1144.
- (23) Liu, G.; Wu, B.; Zhang, J.; Wang, X.; Shao, M.; Wang, J. *Inorg. Chem.* **2009**, *48*, 2383.
- (24) Xing, L.; Xie, J.-H.; Chen, Y.-S.; Wang, L.-X.; Zhou, Q.-L. *Adv. Synth. Catal.* **2008**, *350*, 1013.
- (25) Su, H.; Li, Z.; Huo, Q.; Guan, J.; Kan, Q. *RSC Adv.* **2014**, *4*, 9990.
- (26) (a) Minisci, F.; Fontana, F.; Araneo, S.; Recupero, F.; Banfi, S.; Quici, S. *J. Am. Chem. Soc.* **1995**, *117*, 226. (b) Minisci, F.; Fontana, F.; Araneo, S.; Rupero, F. *J. Chem. Soc., Chem. Commun.* **1994**, 1823. (c) Bravo, A.; Bjørsvik, H.-R.; Fontana, F.; Liguori, L.; Minisci, F. *J. Org. Chem.* **1997**, *62*, 3849. (d) Yu, J.-Q.; Corey, E. *Org. Lett.* **2002**, *4*, 2727.
- (27) Fraile, J. M.; Garcia, J. I.; Herreras, C. I.; Mayoral, J. A.; Pires, E. *Chem. Soc. Rev.* **2009**, *38*, 695.
- (28) Meijer, M.; van Klink, G.; van Koten, G. *Coord. Chem. Rev.* **2002**, *230*, 141.
- (29) (a) Maggini, M.; Guldi, D.; Mondini, S.; Scorrano, G.; Paolucci, F.; Ceroni, P.; Roffia, S. *Chem.—Eur. J.* **1998**, *4*, 1992. (b) Armaroli, N.; Accorsi, G.; Felder, D.; Nierengarten, J.-F. *Chem.—Eur. J.* **2002**, *8*, 2314. (c) Zhou, Z.; Sarova, G.; Zhang, S.; Ou, Z.; Tat, F.; Kadish, K.; Echegoyen, L.; Guldi, D.; Schuster, D.; Wilson, S. *Chem.—Eur. J.* **2006**, *12*, 4241.
- (30) (a) Fu, K.; Henbest, K.; Zhang, Y.; Valentin, S.; Sun, Y.-P. *J. Photochem. Photobiol., A* **2002**, *150*, 143. (b) Gao, Y.; Song, Y.; Li, Y.; Wang, Y.; Liu, H.; Zhu, D. *Appl. Phys. B: Laser Opt.* **2003**, *76*, 761.
- (31) (a) Song, L.-C.; Liu, X.-F.; Xie, Z.-J.; Luo, F.-X.; Song, H.-B. *Inorg. Chem.* **2011**, *50*, 11162. (b) Xu, W.; Feng, L.; Wu, Y.; Wang, T.; Wu, J.; Xiang, J.; Li, B.; Jiang, L.; Shu, C.; Wang, C. *Phys. Chem. Chem. Phys.* **2011**, *13*, 428. (c) D'Souza, F.; Gadde, S.; Islam, S.; Wijesinghe, C.; Schumacher, A.; Zandler, M.; Araki, Y.; Ito, O. *J. Phys. Chem. A* **2007**, *111*, 8552. (d) Vail, S.; Krawczuk, P.; Guldi, D.; Palkar, A.; Echegoyen, L.; Tomé, J.; Fazio, M.; Schuster, D. *Chem.—Eur. J.* **2005**, *11*, 3375. (e) Wijesinghe, C.; El-Khouly, M.; Zandler, M.; Fukuzumi, S.; D'Souza, F. *Chem.—Eur. J.* **2013**, *19*, 9629.